SIAM J. Applied Dynamical Systems
Vol. 21, No. 4, pp. 2518–2534

Periodic Waves of the Modified KdV Equation as Minimizers of a New Variational Problem*

Uyen Le† and Dmitry E. Pelinovsky‡

Abstract. Periodic waves of the modified Korteweg-de Vries (mKdV) equation are identified in the context of a new variational problem with two constraints. The advantage of this variational problem is that its nondegenerate local minimizers are stable in the time evolution of the mKdV equation, whereas the saddle points are unstable. We explore the analytical representation of periodic waves given by Jacobi elliptic functions and compute numerically critical points of the constrained variational problem. A broken pitchfork bifurcation of three smooth solution families is found. Two families represent (stable) minimizers of the constrained variational problem and one family represents (unstable) saddle points.

Key words. modified Korteweg-de Vries equation, periodic waves, energy minimization

MSC codes. 35Q51, 35Q53, 76B25

DOI. 10.1137/21M1465329

1. Introduction.

We address traveling periodic waves of the modified Korteweg-de Vries (mKdV) equation which we take in the normalized form

$$u_t + 6u^2 u_x + u_{xxx} = 0. \tag{1}$$

For the sake of clarity, we normalize the wave period to 2π and denote the Sobolev spaces of 2π-periodic functions by $H^k_{\rm per}$ for $k \in \mathbb{N}$ with $H^0_{\rm per} \equiv L^2_{\rm per}$ for $k = 0$.

Traveling waves of the form $u(t,x) = \psi(x - ct)$ satisfy the stationary equation

$$-\psi'' + c\psi + b = 2\psi^3, \tag{2}$$

where $\psi(x) : [0, 2\pi] \mapsto \mathbb{R}$ is the wave profile, c is the wave speed, and b is the constant of integration. Traveling periodic waves of the mKdV equation (1) play a fundamental role in physical applications, e.g., for dynamics of the internal waves in seas and oceans [12, 21, 22]. A period function for periodic solutions of the stationary equation (2) has been studied in

* Received by the editors December 14, 2021; accepted for publication (in revised form) by T. Ogawa July 26, 2022; published electronically December 5, 2022.
https://doi.org/10.1137/21M1465329
Funding: The work of the first author was supported by a McMaster graduate scholarship. The work of the second author was supported by Ministry of Science and Higher Education of the Russian Federation grant FSWE-2020-0007 and Russian Federation for the leading scientific schools grant NSH-70.2022.1.5.

† Department of Mathematics and Statistics, McMaster University, Hamilton L8S 4K1, ON, Canada, Canada (leu@mcmaster.ca).
‡ Department of Mathematics and Statistics, McMaster University, Hamilton L8S 4K, ON, Canada, Canada and Department of Applied Mathematics, Nizhny Novgorod State Technical University, 24 Minin street, Nizhny Novgorod, Russia (dmpeli@math.mcmaster.ca).

[7, 10, 23]. Stability of periodic waves in the defocusing version of the mKdV equation was studied both with respect to coperiodic and subharmonic perturbations [9]. We consider the focusing version of the mKdV equation (1) and the coperiodic perturbations.

Transformations $\psi(x) = \alpha\tilde{\psi}(\alpha x)$, $c = \alpha^2\tilde{c}$, and $b = \alpha^3\tilde{b}$ leave the stationary equation (2) invariant. Hence, the results obtained for the 2π-periodic solutions are extended to the L-periodic solutions for every $L > 0$ by taking $\alpha := \frac{L}{2\pi}$.

There exist two families of periodic solutions to the stationary equation (2) for $b = 0$: dnoidal waves with sign-definite profile ψ and cnoidal waves with sign-indefinite profile ψ. Spectral and orbital stability of these periodic waves has been explored in the recent literature [3, 4, 8]. While sign-definite dnoidal waves are stable for all speeds, sign-indefinite cnoidal waves are stable for smaller speeds c and unstable for larger speeds c [8].

Compared to these definite results, the stationary mKdV equation (2) with $b \neq 0$ has more general families of periodic waves expressed as two rational functions of Jacobi elliptic functions [6]. Stability of a particular family of positive periodic waves with $b \neq 0$ has been proven in [2], but no general results on stability of these periodic waves are available in the literature to the best of our knowledge. A new variational formulation of the periodic waves with $b \neq 0$ was developed in our previous works with Natali [17, 18] (see also the follow-up work [1]).

The purpose of this paper is to explore the new variational formulation of traveling periodic waves and to detect numerically which periodic waves with $b \neq 0$ are stable and which are unstable in the time evolution of the mKdV equation (1).

Since the mKdV equation (1) admits the following conserved quantities on the 2π-periodic domain,

$$E(u) = \frac{1}{2}\oint \left[(u')^2 - u^4\right] dx, \quad F(u) = \frac{1}{2}\oint u^2 dx, \quad M(u) = \oint u dx, \tag{3}$$

the stationary equation (2) is the Euler-Lagrange equation for the action functional

$$G_{c,b}(u) := E(u) + cF(u) + bM(u). \tag{4}$$

We refer to $E(u)$, $F(u)$, and $M(u)$ as the energy, momentum, and mass, respectively.

The standard variational formulation for stability of periodic waves is to find minimizers of energy $E(u)$ in $H^1_{\rm per}$ subject to the fixed momentum $F(u)$ and mass $M(u)$ [5, 14, 16, 20]. Parameters c and b of the stationary equation (2) are Lagrange multipliers of the action (4). Unfortunately, this formulation may suffer from nonsmooth dependence of the minimizers from Lagrange multipliers (c, b) as discussed in [17, 18] after [15]. This breakdown of the variational theory happens at the bifurcation points for which the Hessian operator for $G_{c,b}(u)$ admits a zero eigenvalue, where $\mathcal{L} = G''_{c,b}(\psi) : H^2_{\rm per} \subset L^2_{\rm per} \mapsto L^2_{\rm per}$ is given by

$$\mathcal{L} = -\partial_x^2 + c - 6\psi^2. \tag{5}$$

In [18] (based on the previous work [17] in the case of quadratic nonlinearities), we have proposed a new variational approach to characterize the periodic waves of the stationary equation (2) as minimizers of the following constrained variational problem,

$$r_{c,m} := \inf_{u \in H^1_{\rm per}} \left\{ \mathcal{B}_c(u) : \quad \oint u^4 dx = 1, \quad \frac{1}{2\pi}\oint u dx = m \right\}, \tag{6}$$

where

$$\mathcal{B}_c(u) := \frac{1}{2} \oint \left[(u')^2 + cu^2 \right] dx. \tag{7}$$

It was shown in [18, Appendix B] that the minimizer exists for every $c \in (-1, \infty)$ and every $m \in [-m_0, m_0]$, where $m_0 := (2\pi)^{-1/4}$. The minimizer has one maximum and one minimum on the 2π-periodic domain if $m \in (-m_0, m_0)$ and is given by the constant solution if $m = \pm m_0$. The minimizer $\chi \in H^1_{\rm per}$ such that $r_{c,m} = \mathcal{B}_c(\chi)$ gives the solution of the stationary equation (2) by using the scaling transformation

$$\psi = \chi \frac{\sqrt{\mathcal{B}_c(\chi) - \pi c m^2}}{\sqrt{1 - m \oint \chi^3 dx}}, \tag{8}$$

and it was shown in [18] that $\mathcal{B}_c(\chi) - \pi c m^2 > 0$ and $1 - m \oint \chi^3 dx > 0$. The inverse transformation is given by $\chi = \psi / \|\psi\|_{L^4}$, hence

$$m = \frac{1}{2\pi \|\psi\|_{L^4}} \oint \psi dx. \tag{9}$$

The family of sign-indefinite cnoidal waves for the stationary equation (2) with $b = 0$ was recovered in [18] from the variational problem (6) for $c \in (-1, \infty)$ and $m = 0$ in the space of odd periodic functions. It was found that the family is smooth with respect to parameter c but there exists a bifurcation point $c_0 \approx 1.425$ such that the sign-indefinite wave is not a minimizer of the variational problem (6) for $c \in (c_0, \infty)$ and $m = 0$. The bifurcation point c_0 coincides with the stability threshold found in [8]. The transition between the stable and unstable cnoidal waves was also confirmed in [5], where the parameter c was normalized to unity but the period L, the momentum $F(\psi)$, and the mass $M(\psi)$ were continued with respect to parameters of the wave profile ψ. The unstable solutions correspond to the region (b) in Figure 3 in [5] and the stable solutions correspond to the region (d).

Similar study in the case of quadratic nonlinearity in [17] also showed that the family of minimizers of the new variational problem for the traveling periodic waves with zero mean remains smooth with respect to the wave speed c.

Another example when stability of periodic waves was studied outside the standard variational theory based on $G_{c,b}(u)$ in (4) can be found in [11] in the framework of the Camassa–Holm equation. An alternative Hamiltonian structure of this equation was used in order to provide smooth continuation of the periodic waves and the stability conclusion.

Let us now explain the organization of this paper.

In section 2, we develop the stability theory for the traveling periodic waves given by nondegenerate local minimizers and saddle points of the variational problem (6). We derive a precise stability criterion for a nondegenerate local minimizer and a precise instability criterion for a saddle point of the variational problem (6).

In section 3, we perform the numerical search of critical points of the variational problem (6). We show that the global minimizers remain smooth in (c, m) for every $c \in (-1, \infty)$ and $m \in (0, m_0)$. Besides the smooth family of global minimizers, there exist two other families of periodic waves in a subset of the region $c \in (-1, \infty)$ and $m \in (0, m_0)$: one family contains local

minimizers and the other family contains saddle points of the variational problem (6). The two families disappear at the fold bifurcation point $c_*(m)$. When $m \to 0$, $c_*(m) \to c_0 \approx 1.425$, where the three families are connected in the pitchfork bifurcation observed in [18]. No other solution families have been identified in the numerical search.

Computing the stability criterion numerically, we show that the two families of minimizers are stable in the time evolution of the mKdV equation (1) whereas the only family of saddle points is unstable. These results generalize the result of [18] obtained for $m = 0$.

Section 4 concludes the paper with a summary and a discussion of further questions.

2. Stability theory for nondegenerate critical points. Let $\chi \in H^1_{\rm per}$ be a minimizer of the variational problem (6) for $c \in (-1, \infty)$ and $m \in (0, m_0)$ which always exists by Proposition 6.5 in [18]. Let $\psi \in H^1_{\rm per}$ be obtained by means of the transformation (8). Then, ψ satisfies the stationary equation (2) with uniquely defined function

$$b = b(c, m) := \frac{1}{\pi} \oint \psi^3 dx - cm\|\psi\|_{L^4}. \tag{10}$$

The profile ψ has exactly one maximum and one minimum point on the 2π-periodic domain. The main assumption on the minimizer χ is given as follows.

> Assume that χ is a nondegenerate minimizer of the variational problem (6) module to the translational symmetry: $\chi(x) \mapsto \chi(x + x_0)$ for every $x_0 \in \mathbb{R}$.

For the solution ψ of the stationary equation (2) given by (8), this assumption implies that the Hessian operator $\mathcal{L}$ in (5) restricted to the orthogonal complement of $\{1, \psi^3\}$ in $L^2_{\rm per}$ is positive and admits a simple zero eigenvalue with the eigenfunction $\partial_x \psi$. For the sake of notations, we denote the restriction of $\mathcal{L}$ to $\{1, \psi^3\}^\perp$ in $L^2_{\rm per}$ by $\mathcal{L}|_{\{1,\psi^3\}^\perp}$. With the standard notations of $n(\mathcal{L})$ and $z(\mathcal{L})$ for the number of negative eigenvalues and the multiplicity of the zero eigenvalue of a self-adjoint operator $\mathcal{L}$, we express the main assumption in the form

$$n(\mathcal{L}|_{\{1,\psi^3\}^\perp}) = 0, \quad z(\mathcal{L}|_{\{1,\psi^3\}^\perp}) = 1. \tag{11}$$

By using the implicit function argument (similar to Lemma 2.8 in [18]), it is easy to prove that the assumption (11) implies smoothness of a continuation of the periodic waves with the profile $\psi \in H^1_{\rm per}|_{\{1\}^\perp}$ with respect to parameters (c, m) such that $\partial_c \psi$ and $\partial_m \psi$ are 2π-periodic. This implies with the help of (10) that the function b is also smooth in (c, m). Hence, both $\psi \in H^1_{\rm per}$ and b can be differentiated in (c, m), from which we can characterize the range of $\mathcal{L}$ by using

$$\mathcal{L}1 = c - 6\psi^2, \tag{12}$$

$$\mathcal{L}\psi = -b - 4\psi^3, \tag{13}$$

$$\mathcal{L}\partial_c \psi = -\partial_c b - \psi, \tag{14}$$

$$\mathcal{L}\partial_m \psi = -\partial_m b. \tag{15}$$

We recall from [15] (see also Proposition 2.5 in [18]) that $\mathrm{Ker}(\mathcal{L}) = \mathrm{span}(\partial_x \psi)$ if and only if $\{1, \psi, \psi^2\} \in \mathrm{Range}(\mathcal{L})$. By using this result, it follows from (12), (14), and (15) that $z(\mathcal{L}) = 1$ if and only if $\partial_m b \neq 0$.

We also recall that since $\partial_x \psi$ has exactly two zeros on the 2π-periodic domain, Sturm's nodal theory from [15] (see also Proposition 2.4 in [18]) implies that $\mathcal{L}$ is not positive and admits at least one negative eigenvalue: $n(\mathcal{L}) \geq 1$. Since ψ is related to a minimizer of the variational problem (6) with two constraints, we have $1 \leq n(\mathcal{L}) \leq 2$.

Next we count $n(\mathcal{L})$ based on the standard count of eigenvalues of a self-adjoint operator under two orthogonal constraints (see Lemma 2.13 in [18] and Theorem 4.1 in [19]). We compute the limit $\lambda \to 0$ of the following matrix:

$$P(\lambda) := \begin{bmatrix} \langle (\mathcal{L} - \lambda I)^{-1} \psi^3, \psi^3 \rangle & \langle (\mathcal{L} - \lambda I)^{-1} \psi^3, 1 \rangle \\ \langle (\mathcal{L} - \lambda I)^{-1} 1, \psi^3 \rangle & \langle (\mathcal{L} - \lambda I)^{-1} 1, 1 \rangle \end{bmatrix}, \quad \lambda \notin \sigma(\mathcal{L}). \tag{16}$$

If $\partial_m b \neq 0$, it follows from (13) and (15) that

$$\begin{aligned}
\langle \mathcal{L}^{-1} 1, 1 \rangle &= -\frac{1}{\partial_m b} \partial_m \left(\oint \psi dx \right), \\
\langle \mathcal{L}^{-1} 1, \psi^3 \rangle &= -\frac{1}{4 \partial_m b} \partial_m \left(\oint \psi^4 dx \right), \\
\langle \mathcal{L}^{-1} \psi^3, 1 \rangle &= -\frac{1}{4} \oint \psi dx - \frac{b}{4} \langle \mathcal{L}^{-1} 1, 1 \rangle, \\
\langle \mathcal{L}^{-1} \psi^3, \psi^3 \rangle &= -\frac{1}{4} \oint \psi^4 dx - \frac{b}{4} \langle \mathcal{L}^{-1} 1, \psi^3 \rangle,
\end{aligned}$$

which yields

$$\begin{aligned}
\lim_{\lambda \to 0} \det(P(\lambda)) &= \langle \mathcal{L}^{-1} \psi^3, \psi^3 \rangle \, \langle \mathcal{L}^{-1} 1, 1 \rangle - \langle \mathcal{L}^{-1} \psi^3, 1 \rangle \, \langle \mathcal{L}^{-1} 1, \psi^3 \rangle \\
&= \frac{1}{4 \partial_m b} \left[\left(\oint \psi^4 dx \right) \partial_m \left(\oint \psi dx \right) - \frac{1}{4} \left(\oint \psi dx \right) \partial_m \left(\oint \psi^4 dx \right) \right] \\
&= \frac{1}{4 \partial_m b} \left(\oint \psi^4 dx \right)^{\frac{5}{4}} \partial_m \left(\frac{\oint \psi dx}{\left(\oint \psi^4 dx \right)^{\frac{1}{4}}} \right) \\
&= \frac{\pi}{2 \partial_m b} \| \psi \|_{L^4}^5,
\end{aligned}$$

where the relation (9) has been used. Thus, we conclude that the sign of $\lim_{\lambda \to 0} \det(P(\lambda))$ coincides with the sign of $\partial_m b$.

Recall the counting formulas (see Proposition 2.12 in [18]),

$$\begin{cases} n(\mathcal{L}|_{\{1, \psi^3\}^\perp}) = n(\mathcal{L}) - n_0 - z_0 = 0, \\ z(\mathcal{L}|_{\{1, \psi^3\}^\perp}) = z(\mathcal{L}) + z_0 - z_\infty = 1, \end{cases} \tag{17}$$

where z_0 is the multiplicity of the zero eigenvalue of $\lim_{\lambda \to 0} P(\lambda)$, n_0 is the number of negative eigenvalues of $\lim_{\lambda \to 0} P(\lambda)$, and z_∞ is the number of eigenvalues $P(\lambda)$ diverging to infinity as $\lambda \to 0$.

- If $\partial_m b < 0$, then $\lim_{\lambda\to 0} P(\lambda)$ has one negative eigenvalue so that $n_0 = 1$, $z_0 = z_\infty = 0$ implying from (17) that $n(\mathcal{L}) = 1$ and $z(\mathcal{L}) = 1$.
- If $\partial_m b > 0$, then $\lim_{\lambda\to 0} P(\lambda)$ is either positive or negative, but the former case would imply from (17) that $\mathcal{L}$ is positive, in contradiction with $n(\mathcal{L}) \geq 1$. Hence $\lim_{\lambda\to 0} P(\lambda)$ is negative with $n_0 = 2$, $z_0 = z_\infty = 0$ implying from (17) that $n(\mathcal{L}) = 2$ and $z(\mathcal{L}) = 1$.
- If $\partial_m b = 0$, then $z_\infty = 1$, $z_0 = 0$ implying from (17) that $z(\mathcal{L}) = 2$. This suggests that one of the two negative eigenvalues of $\lim_{\lambda\to 0} P(\lambda)$ for $\partial_m b > 0$ diverges to infinity as $\partial_m b \to 0$, whereas the other eigenvalue of $\lim_{\lambda\to 0} P(\lambda)$ remains negative so that $n_0 = 1$ and $n(\mathcal{L}) = 1$.

These computations are summarized as follows:

$$n(\mathcal{L}) = \begin{cases} 2 & \text{if } \partial_m b > 0, \\ 1 & \text{if } \partial_m b \leq 0, \end{cases} \qquad z(\mathcal{L}) = \begin{cases} 2 & \text{if } \partial_m b = 0, \\ 1 & \text{if } \partial_m b \neq 0. \end{cases} \tag{18}$$

Next we determine the stability of minimizers in the time evolution of the mKdV equation (1) by computing $n(\mathcal{L}|_{\{1,\psi\}^\perp})$ and $z(\mathcal{L}|_{\{1,\psi\}^\perp})$ and by using the stability criteria from [14]:

- The periodic wave with profile ψ is stable if

$$n(\mathcal{L}|_{\{1,\psi\}^\perp}) = 0 \qquad \text{and} \qquad z(\mathcal{L}|_{\{1,\psi\}^\perp}) = 1. \tag{19}$$

- The periodic wave with profile ψ is unstable if

$$n(\mathcal{L}|_{\{1,\psi\}^\perp}) = 1 \qquad \text{and} \qquad z(\mathcal{L}|_{\{1,\psi\}^\perp}) = 1. \tag{20}$$

Similarly to Theorem 2.14 in [18], we compute the limit $\lambda \to 0$ of the following matrix:

$$D(\lambda) := \begin{bmatrix} \langle (\mathcal{L} - \lambda I)^{-1}\psi, \psi\rangle & \langle (\mathcal{L} - \lambda I)^{-1}\psi, 1\rangle \\ \langle (\mathcal{L} - \lambda I)^{-1}1, \psi\rangle & \langle (\mathcal{L} - \lambda I)^{-1}1, 1\rangle \end{bmatrix}, \quad \lambda \notin \sigma(\mathcal{L}). \tag{21}$$

If $\partial_m b \neq 0$, it follows from (14) and (15) that

$$\begin{aligned} \langle \mathcal{L}^{-1}1, 1\rangle &= -\frac{1}{\partial_m b}\partial_m \left(\oint \psi dx \right), \\ \langle \mathcal{L}^{-1}1, \psi\rangle &= -\frac{1}{2\partial_m b}\partial_m \left(\oint \psi^2 dx \right), \\ \langle \mathcal{L}^{-1}\psi, 1\rangle &= -\partial_c \left(\oint \psi dx \right) - \partial_c b \, \langle \mathcal{L}^{-1}1, 1\rangle, \\ \langle \mathcal{L}^{-1}\psi, \psi\rangle &= -\frac{1}{2}\partial_c \left(\oint \psi^2 dx \right) - \partial_c b \, \langle \mathcal{L}^{-1}1, \psi\rangle, \end{aligned}$$

which yields

$$\begin{aligned} \lim_{\lambda\to 0} \det(D(\lambda)) &= \langle \mathcal{L}^{-1}\psi, \psi\rangle \, \langle \mathcal{L}^{-1}1, 1\rangle - \langle \mathcal{L}^{-1}\psi, 1\rangle \, \langle \mathcal{L}^{-1}1, \psi\rangle \\ &= \frac{1}{2\partial_m b}\left[\partial_c \left(\oint \psi^2 dx \right) \partial_m \left(\oint \psi dx \right) - \partial_m \left(\oint \psi^2 dx \right) \partial_c \left(\oint \psi dx \right) \right] \\ &= \frac{1}{2\partial_m b} \begin{vmatrix} \partial_c \mathcal{F}(c,m) & \partial_m \mathcal{F}(c,m) \\ \partial_c \mathcal{M}(c,m) & \partial_m \mathcal{M}(c,m) \end{vmatrix}, \end{aligned}$$

where $\mathcal{F}(c,m) := F(\psi)$ and $\mathcal{M}(c,m) := M(\psi)$ are computed from the two conserved quantities in (3) at the family of periodic waves with the profile ψ that depends on parameters (c,m). Note that the determinant in the last expression is the Jacobian of the transformation $(c,m) \mapsto (\mathcal{F},\mathcal{M})$.

We shall now use the counting formulas,

$$\begin{cases} n(\mathcal{L}|_{\{1,\psi\}^\perp}) = n(\mathcal{L}) - n_0 - z_0, \\ z(\mathcal{L}|_{\{1,\psi\}^\perp}) = z(\mathcal{L}) + z_0 - z_\infty, \end{cases} \tag{22}$$

where z_0, n_0, and z_∞ have the same meaning as in (17) but for the matrix $D(\lambda)$.

- If $\partial_m b < 0$, then it follows from (18) that $n(\mathcal{L}) = 1$ and $z(\mathcal{L}) = 1$ so that the stability criterion (19) is satisfied if and only if $n_0 = 1$, $z_0 = z_\infty = 0$, which is true if and only if the Jacobian of the transformation $(c,m) \mapsto (\mathcal{F},\mathcal{M})$ is strictly positive.
- If $\partial_m b > 0$, then it follows from (18) that $n(\mathcal{L}) = 2$ and $z(\mathcal{L}) = 1$ so that the stability criterion (19) is satisfied if and only if $n_0 = 2$, $z_0 = z_\infty = 0$, that is, $\langle \mathcal{L}^{-1}1, 1\rangle < 0$ and the Jacobian of the transformation $(c,m) \mapsto (\mathcal{F},\mathcal{M})$ is strictly positive. Since $\langle \mathcal{L}^{-1}1, 1\rangle$ is the same diagonal term of both $\lim\limits_{\lambda\to 0} P(\lambda)$ and $\lim\limits_{\lambda\to 0} D(\lambda)$ whereas the former is strictly negative, the first condition of $\langle \mathcal{L}^{-1}1, 1\rangle < 0$ is satisfied.
- If $\partial_m b = 0$, then it follows from (18) that $n(\mathcal{L}) = 1$ and $z(\mathcal{L}) = 2$ so that $\det D(\lambda)$ is singular in the limit $\lambda \to 0$. Hence $z_\infty = 1$ and one of the two negative eigenvalues of $\lim\limits_{\lambda\to 0} D(\lambda)$ for $\partial_m b > 0$ diverges to infinity as $\partial_m b \to 0$, whereas the other eigenvalue of $\lim\limits_{\lambda\to 0} D(\lambda)$ remains negative if and only if the Jacobian of the transformation $(c,m) \mapsto (\mathcal{F},\mathcal{M})$ is strictly positive, which implies $n_0 = 1$, $z_0 = 0$, and hence the stability criterion (19).

The stability criterion in all three cases can be summarized as follows.

Let $\psi \in H^1_{\rm per}$ be a solution of the stationary equation (2) satisfying (11). The periodic wave with the profile ψ is stable in the time evolution of the mKdV equation (1) if

$$\begin{vmatrix} \partial_c \mathcal{F}(c,m) & \partial_m \mathcal{F}(c,m) \\ \partial_c \mathcal{M}(c,m) & \partial_m \mathcal{M}(c,m) \end{vmatrix} > 0. \tag{23}$$

Note that the assumption (11) is satisfied for the solution $\psi \in H^1_{\rm per}$ related to both the global and local nondegenerate minimizers $\chi \in H^1_{\rm per}$ of the variational problem (6).

Let us now consider the nondegenerate saddle points under the following assumption.

Assume that χ is a nondegenerate saddle point of the variational problem (6) module to the translational symmetry: $\chi(x) \mapsto \chi(x + x_0)$ for every $x_0 \in \mathbb{R}$ with exactly one negative direction in $H^1_{\rm per}$ under the two constraints.

The main assumption for the corresponding solution $\psi \in H^1_{\rm per}$ of the stationary equation (2) can be expressed in the form

$$n(\mathcal{L}|_{\{1,\psi^3\}^\perp}) = 1, \quad z(\mathcal{L}|_{\{1,\psi^3\}^\perp}) = 1. \tag{24}$$

The nondegeneracy of the saddle point implies smoothness of $\psi \in H^1_{\rm per}$ and b with respect to parameters (c, m). As a result, the same count of $n(\mathcal{L})$ can be performed based on $\lim P(\lambda)$ with exactly the same expression for $\lim_{\lambda\to 0} \det(P(\lambda))$ if $\partial_m b \neq 0$. Since $\lim_{\lambda\to 0} \det(P(\lambda)) \neq 0$, it follows from (17) with $z_0 = z_\infty = 0$ that $n(\mathcal{L}) = 2$ if $\partial_m b < 0$ for which $n_0 = 1$. Since $1 \leq n(\mathcal{L}) \leq 2$ is no longer true for the saddle points, the case with $\partial_m b > 0$ may either give $n(\mathcal{L}) = 1$ or $n(\mathcal{L}) = 3$. To avoid ambiguity, we only consider the saddle points with $\partial_m b < 0$.

It follows from (22) that if $\partial_m b < 0$, then the instability criterion (20) is satisfied if and only if the Jacobian of the transformation $(c, m) \mapsto (\mathcal{F}, \mathcal{M})$ is strictly positive for which $n_0 = 1$, $z_0 = z_\infty = 0$. The instability criterion can be summarized as follows.

Let $\psi \in H^1_{\rm per}$ be a solution of the stationary equation (2) satisfying (24). The periodic wave with the profile ψ is unstable in the time evolution of the mKdV equation (1) if $\partial_m b < 0$ and

$$\begin{vmatrix} \partial_c \mathcal{F}(c,m) & \partial_m \mathcal{F}(c,m) \\ \partial_c \mathcal{M}(c,m) & \partial_m \mathcal{M}(c,m) \end{vmatrix} > 0. \tag{25}$$

Although the stability and instability criteria (23) and (25) are only sufficient conditions, we show with the help of numerical approximations that these criteria cover all critical points of the variational problem (6).

3. Numerical search of critical points of the variational problem. To perform the numerical search, we use the analytical representation of solutions to the stationary equation (2) in terms of the Jacobi elliptic functions. Such representations are known in the literature; we refer to [6] for precise details.

One family of exact solutions is given by

$$\psi(x) = u_4 + \frac{(u_1 - u_4)(u_2 - u_4)}{(u_2 - u_4) + (u_1 - u_2)\,\mathrm{sn}^2(\nu x; k)}, \tag{26}$$

where the turning points u_1, u_2, u_3, u_4 satisfy the constraint

$$u_1 + u_2 + u_3 + u_4 = 0 \tag{27}$$

and define parameters c and b of the stationary equation (2) by

$$\begin{cases} c = -(u_1u_2 + u_1u_3 + u_1u_4 + u_2u_3 + u_2u_4 + u_3u_4), \\ b = \frac{1}{2}(u_1u_2u_3 + u_1u_2u_4 + u_1u_3u_4 + u_2u_3u_4). \end{cases} \tag{28}$$

Parameters ν and k of the solution (26) are expressed by the relations

$$\nu = \frac{1}{2}\sqrt{(u_1 - u_3)(u_2 - u_4)}, \quad k = \frac{\sqrt{(u_1 - u_2)(u_3 - u_4)}}{\sqrt{(u_1 - u_3)(u_2 - u_4)}}.$$

When a given value of $c \in (-1,\infty)$ is substituted into the first equation in (28) and the additional constraint (27) is used, the family of solutions (26) has two arbitrary parameters among the four turning points, which we choose to be u_1 and u_2. These two parameters are defined from two additional constraints: the period of ψ must be normalized to 2π by $2K(k) = 2\pi\nu$, where $K(k)$ is the complete elliptic integral, and the mean value and the L^4 norm of the solution ψ must be related to a given value of $m \in (-m_0, m_0)$ by (9). Newton's method is used to satisfy these two constraints and to find the admissible values of u_1 and u_2. The function $b = b(c,m)$ is computed from the second equation in (28).

Another family of exact solutions is given by

$$\psi(x) = u_1 + \frac{(u_2-u_1)(1-\ \mathrm{cn}(\nu x;k))}{1-\ \mathrm{cn}(\nu x;k) + \delta(1+\ \mathrm{cn}(\nu x;k))} \tag{29}$$

with the turning points u_1, u_2, $u_3 = \alpha + i\beta$, $u_4 = \alpha - i\beta$. The turning points satisfy the constraint

$$u_1 + u_2 + 2\alpha = 0 \tag{30}$$

and define parameters c and b of the stationary equation (2) by

$$\begin{cases} c = -(u_1u_2 + 2\alpha(u_1+u_2) + \alpha^2 + \beta^2), \\ b = \alpha u_1 u_2 + \frac{1}{2}(u_1+u_2)(\alpha^2+\beta^2). \end{cases} \tag{31}$$

Parameters ν, k, and δ of the solution (29) are expressed by the relations

$$\delta = \frac{\sqrt{(u_2-\alpha)^2+\beta^2}}{\sqrt{(u_1-\alpha)^2+\beta^2}}, \quad \nu = \sqrt[4]{[(u_1-\alpha)^2+\beta^2]\,[(u_2-\alpha)^2+\beta^2]},$$

and

$$k = \frac{1}{\sqrt{2}}\sqrt{1 - \frac{(u_1-\alpha)(u_2-\alpha)+\beta^2}{\sqrt{(u_1-\alpha)^2+\beta^2}\sqrt{(u_2-\alpha)^2+\beta^2}}}.$$

Again we use (30) to define α and the first equation in (31) to define β from $c \in (-1,\infty)$. The remaining parameters u_1 and u_2 are computed from two additional constraints: the period of ψ must be normalized to 2π by $4K(k) = 2\pi\nu$ and the mean value and the L^4 norm of the solution ψ must be related to a given value of $m \in (-m_0, m_0)$ by (9). Newton's method is used to satisfy these two constraints for u_1 and u_2, from which we obtain the function $b = b(c,m)$ from the second equation in (31).

Figure 1 presents the main result in obtaining numerical solutions from the exact solutions (26) and (29) with parameters found from Newton's method for $c \in (-1,\infty)$ and $m \in [0, m_0)$. Three solution families are shown for b versus c for fixed values of m. The solid curves represent solutions of the form (29) and the dotted curves are solutions of the form (26). The black and blue dots demark the points at which the two solution forms connect. Continuing one solution form across these points is impossible because the elliptic modulus k becomes complex valued. The red dot shows pitchfork bifurcation (for $m = 0$) and fold bifurcation (for $m \neq 0$) when the solution families coalesce.

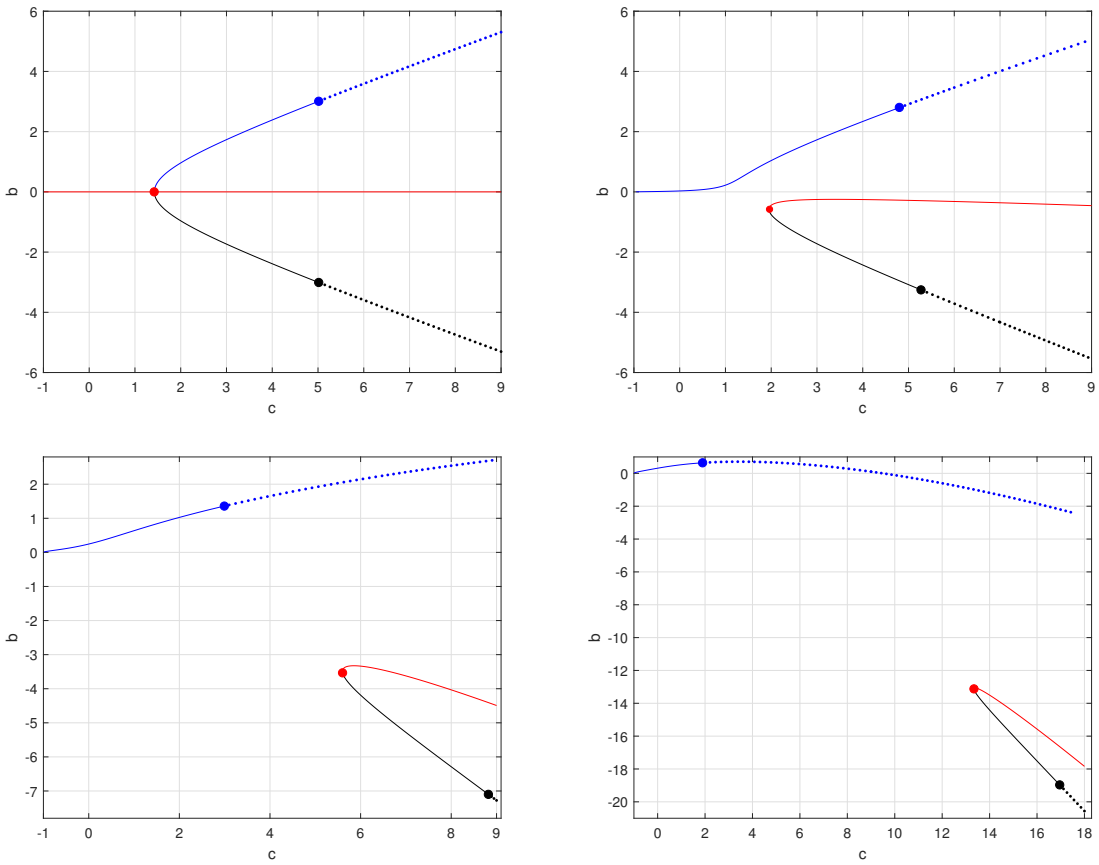

Figure 1. *Three solution families on the (b, c) diagram for fixed values of m: $m = 0$ (top left), $m = 0.01$ (top right), $m = 0.1$ (bottom left), and $m = 0.2$ (bottom right).*

Figure 1 (top left) agrees with Figure 2 (middle left panel) in [18] obtained from numerical solutions of the stationary equation (2). For $m = 0$, there exists $c_0 \approx 1.425$ (red dot) at which the pitchfork bifurcation occurs. For $m \neq 0$ in Figure 1, the symmetry is broken, the bifurcation point $c_*(m)$ such that $c_*(m) \to c_0$ as $m \to 0$ detaches from the upper branch but remains the connection point for the middle and lower solution families. As m increases, $c_*(m)$ at the bifurcation point increases rapidly and the two solution families move to larger values of c.

Figure 2 (left) shows only the upper solution family on the (b, c) plane but for larger values of m compared to Fig. 1. Figure 2 (right) compares the numerical result for $m = 0.6$ with the analytical result for $m = m_0 \approx 0.6316$ for which the solution family for the constant solutions is given in the parametric form

$$\begin{cases} c = 6u_1^2 - 1, \\ b = u_1 - 4u_1^3, \end{cases} \qquad u_1 \in (0, \infty). \tag{32}$$

This exact solution for $m = m_0$ follows from either (26) or (29) with $u_2 = u_1$. Although we do not distinguish between the two solution forms (26) and (29) in the same solid lines on

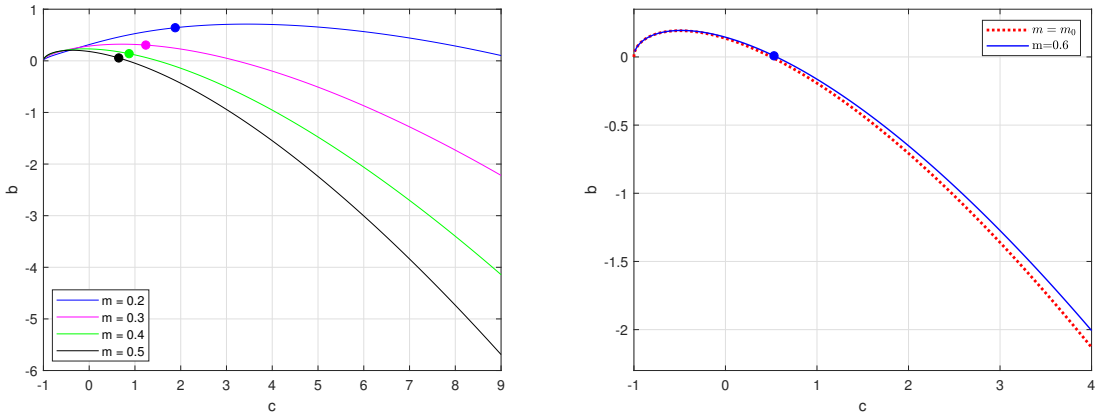

Figure 2. *(Left) The same as Figure 1 but for the upper solution family only for* $m = 0.2, 0.3, 0.4, 0.5$. *(Right) Comparison between the upper solution family for* $m = 0.6$ *and the exact solution for* $m = m_0$.

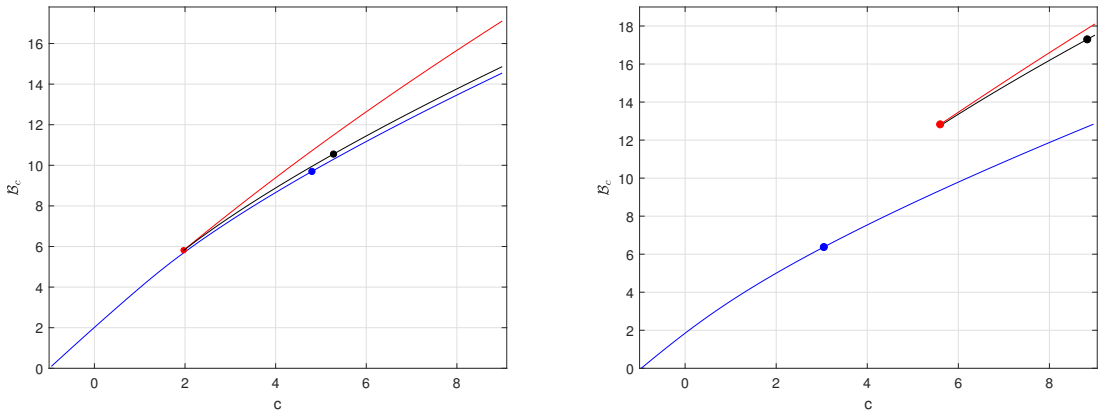

Figure 3. *The value of* $\mathcal{B}_c(\chi)$ *for the three critical points of the variational problem* (6) *versus* c *for two values of* m: $m = 0.01$ *(left) and* $m = 0.1$ *(right).*

Figure 2, the connection point between the two solutions is shown and it moves to smaller values of c as m increases.

Figure 3 clarifies the meaning of each of the three solution families among the critical points of the variational problem (6). It shows the values of $\mathcal{B}_c(\chi)$ defined in (7) versus c for fixed values of $m = 0.01$ (left) and $m = 0.1$ (right), where χ is computed from ψ by using $\chi = \psi/\|\psi\|_{L^4}$. To compute $\mathcal{B}_c(\chi)$, we use forward finite difference to approximate χ' and then complete the quadrature using the trapezoidal rule. In both panels, the blue, red, and black curves correspond, respectively, to the upper, middle, and lower families of solutions at the bifurcation diagrams of Figure 1. We observe that the blue curves represent the global minimizers, the black curves represent the local minimizers, and the red curves represent the saddle points. The numerical search shows that no other solutions of the stationary equation (2) yield critical points of the variational problem (6).

In order to apply the stability criterion (23) for nondegenerate minimizers of the variational problem (6), we glue individual computations together and represent the solution surface of $b = b(c, m)$ versus (c, m) on Figure 4.

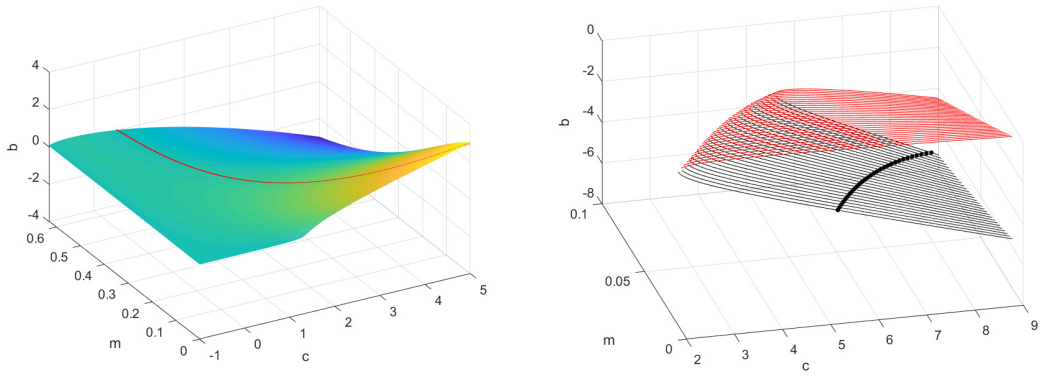

Figure 4. *(Left) The solution surface of $b(c, m)$ for the global minimizers of the variational problem (6). (Right) Two solution surfaces of $b(c, m)$ for the local minimizers and saddle points of the variational problem (6) which connect at the fold bifurcation.*

Figure 4 (left) shows the smooth solution surface for the global minimizers of the variational problem (6) given by the upper solution family on Figure 1 for $c \in (-1, \infty)$ and $m \in (0, m_0)$. It suggests nondegeneracy of the global minimizers except at the point of the fold bifurcation for $m = 0$ and $c = c_0 \approx 1.425$. The red curve on the solution surface in denotes the connection line between the two solution forms (26) and (29).

Figure 4 (right) shows the solution surface $b(m, c)$ for the other two critical points of the variational problem (6). The top (red) part of the surface corresponds to the saddle points and the bottom (black) part of the surface relates to the local minimizers. The numerical result also suggests that the surface is smooth except at the points of the fold bifurcation where the saddle points connect with the local minimizers. The black line denotes the connection line between the two solution forms (26) and (29).

3.1. Stability of the global minimizers. It follows from (18) that the Morse index $n(\mathcal{L})$ and the degeneracy index $z(\mathcal{L})$ depend on the derivative $\partial_m b$. Figure 5 shows $b = b(c, m)$ versus m for fixed values of c. For $m = 0$, the derivative $\partial_m b$ changes sign from positive to negative at $c_1 \approx 3.1$. According to (18), it corresponds to the change in the Morse index $\mathcal{L}$ from $n(\mathcal{L}) = 2$ for $c \in (-1, c_1)$ to $n(\mathcal{L}) = 1$ for $c \in (c_1, \infty)$. This agrees with Figure 2 (bottom left panel) in [18].

It follows from Figure 5 that there exists $m_1(c)$ for $c \in (-1, c_1)$ such that $n(\mathcal{L}) = 2$ for $m \in (0, m_1(c))$ and $n(\mathcal{L}) = 1$ for $m \in (m_1(c), m_0)$. Because $z(\mathcal{L}) = 2$ at $m = m_1(c)$, the nondegeneracy assumption used in the conventional stability theory for periodic waves (see [15, 17] and references therein) is not satisfied at $m = m_1(c)$. In particular, minimizers of energy $E(u)$ for fixed momentum $F(u)$ and mass $M(u)$ are not smooth with respect to parameters (c, b) at the degeneracy point. This drawback of the conventional stability theory is not present for the minimizers of the new variational problem (6).

Figures 6 and 7 show, respectively, the mass $\mathcal{M}(c, m)$ and the momentum $\mathcal{F}(c, m)$ versus c at different values of m (top) and versus m at different values of c (bottom). It is clear that the mass $\mathcal{M}(c, m)$ is monotonically increasing in both c and m, whereas the momentum

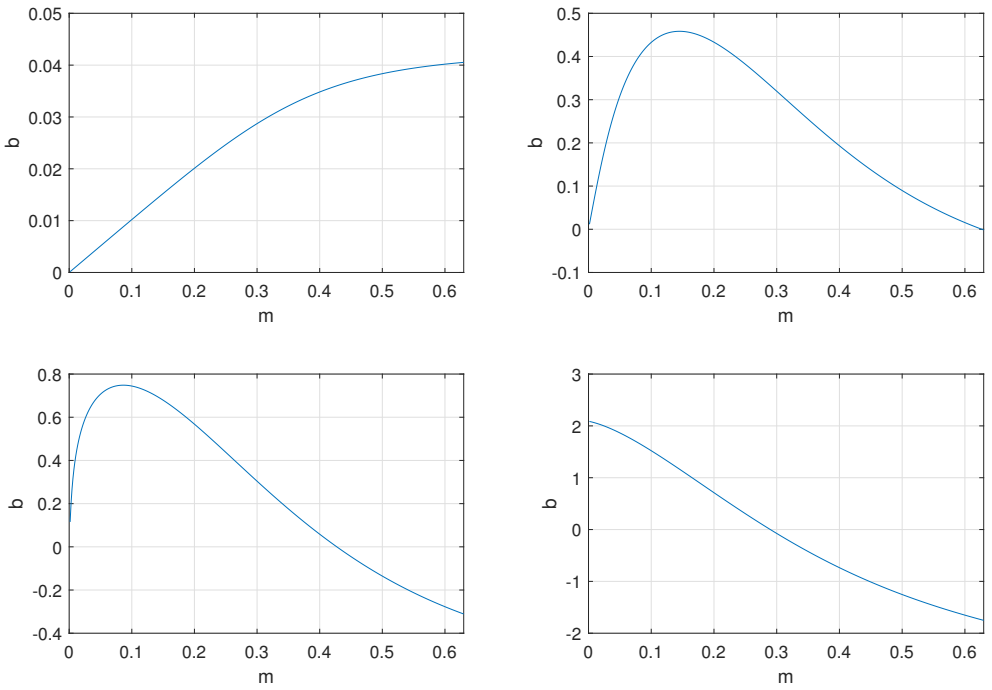

Figure 5. *$b = b(c, m)$ versus m at the solution surface of Fig. 4 (left) for various values of $c = -0.99$ (top left), $c = 0.51$ (top right), $c = 1.26$ (bottom left), and $c = 3.53$ (bottom right).*

$\mathcal{F}(c, m)$ is monotonically increasing in c for every $m \in (0, m_0)$ and monotonically decreasing in m for every $c \in (0, c_0)$, where c_0 is the same bifurcation value of c for the pitchfork bifurcation at $m = 0$. With these signs of partial derivatives, the stability condition (23) is always satisfied for $c \in (0, c_0)$ and $m \in (0, m_0)$. Note that for $m = 0$, we have $\partial_m \mathcal{F}(c, 0) = 0$ and $\partial_m \mathcal{M}(c, 0) > 0$ so that the stability criterion (23) reduces to $\partial_c \mathcal{F}(c, 0) > 0$, monotonicity of the mapping $c \mapsto \mathcal{F}(c, 0)$, which was the main stability criterion used in [17] and [18].

It follows from Figure 7 that for $c > c_0$, there exists $m_*(c) \in (0, m_0)$ such that the momentum $\mathcal{F}(c, m)$ is monotonically decreasing in m for $m \in (0, m_*(c))$ and monotonically increasing in m for $m \in (m_*(c), m_0)$. It is not obvious in the latter case if the stability criterion (23) is satisfied. Figure 8 shows the contour plot for the Jacobian in (23) for all $c \in (-1, 5)$ and $m \in (0, m_0)$, which is strictly positive with the minimal value of 0.0145 attained at the corner point shown by the red dot. Therefore, the stability criterion (23) is satisfied for every nondegenerate minimizer of the variational problem (6).

3.2. Instability of saddle points. Saddle points of the variational problem (6) corrrespond to the middle solution family on Figure 1. The solution surface for the saddle point connects to the solution surface for the local minimizers according to Figure 4 (right).

The instability criterion for the saddle points (25) was derived under the assumption of $\partial_m b < 0$. Figure 9 shows $b = b(c, m)$ versus m for two values of c, which suggests that $\partial_m b < 0$ is satisfied for all saddle points of the variational problem (6).

We have found numerically that the mass $\mathcal{M}(c, m)$ of the saddle points is monotonically increasing in both m and c similarly to Figure 6 for the global minimizers. We also found that

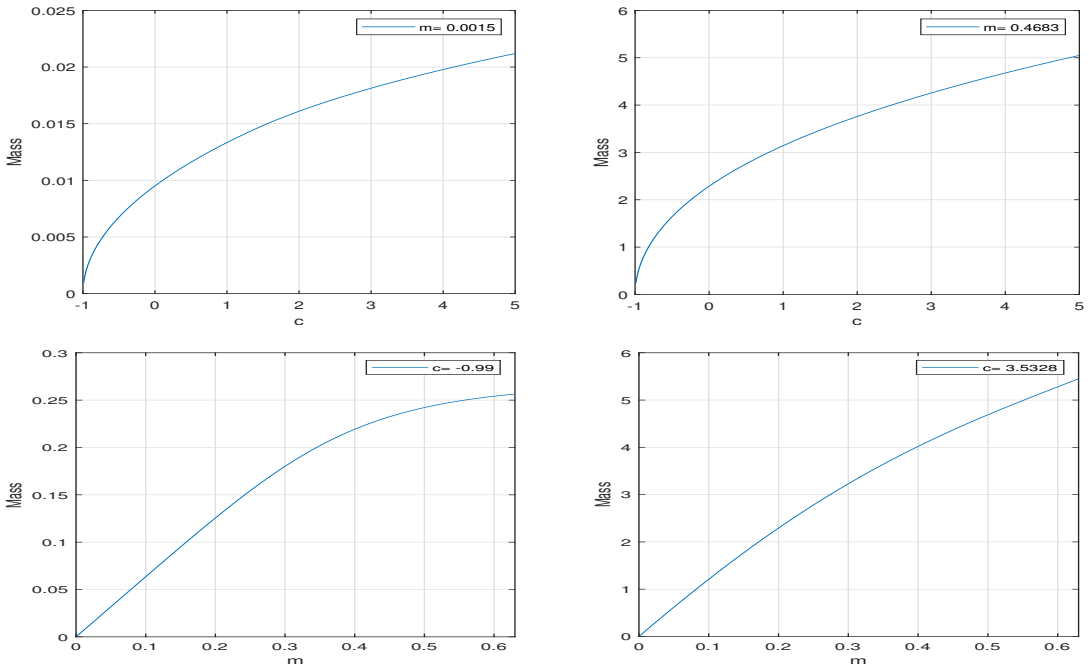

Figure 6. *Top: Mass $\mathcal{M}(c,m)$ versus c for various values of m. Bottom: Mass $\mathcal{M}(c,m)$ versus m for various values of c.*

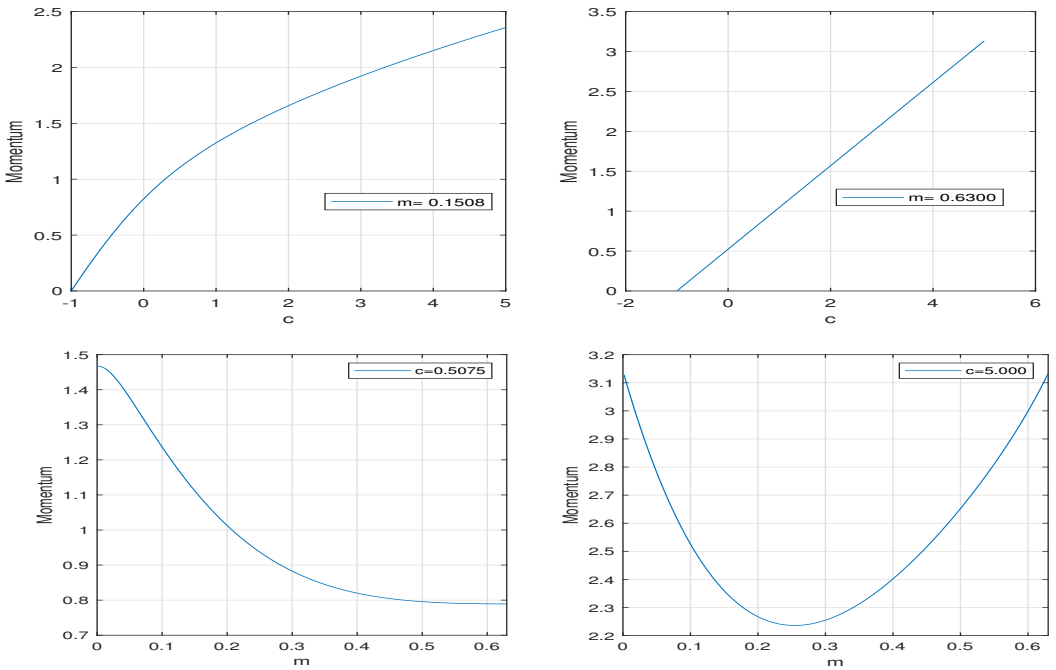

Figure 7. *Top: Momentum $\mathcal{F}(c,m)$ versus c for various values of m. Bottom: Momentum $\mathcal{F}(c,m)$ versus m for various values of c.*

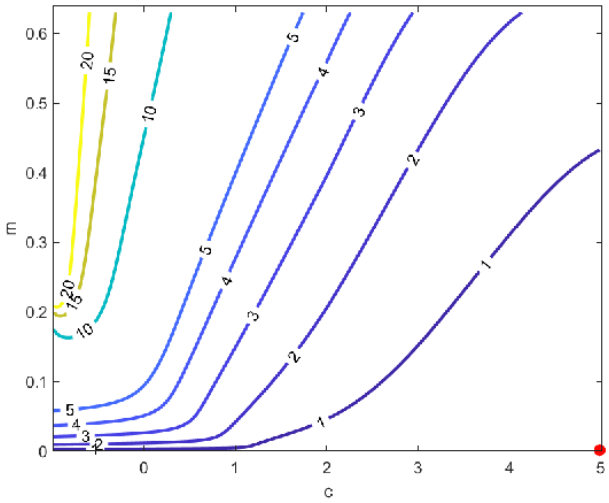

Figure 8. *Contour plot of the Jacobian in the stability criterion* (23) *for the global minimizers.*

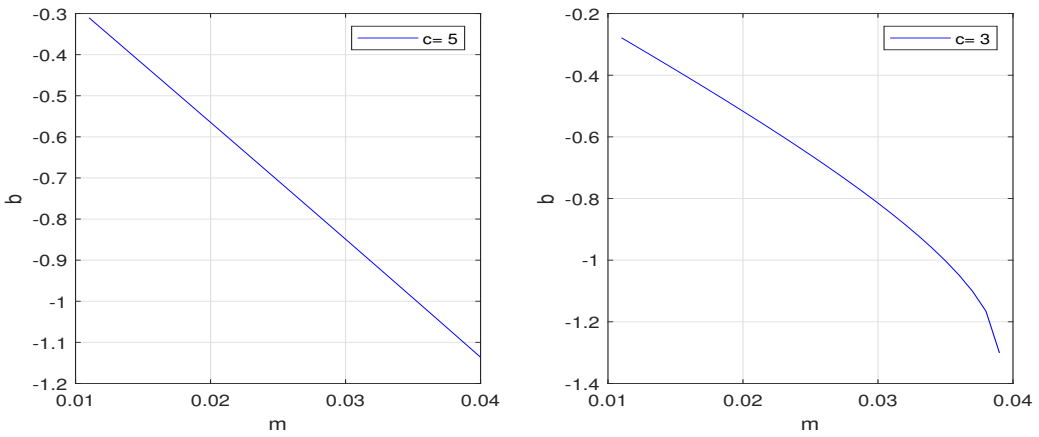

Figure 9. $b = b(c, m)$ *versus* m *for the solution surface of Fig.* 4 *(right) for* $c = 5$ *(left) and* $c = 3$ *(right).*

the momentum $\mathcal{F}(c, m)$ is monotonically increasing in c but there exist c_1 and c_2 satisfying $3 < c_1 < c_2 < 9$ such that $\mathcal{F}(c, m)$ is monotonically decreasing in m for $c < c_1$ and monotonically increasing in m for $c > c_2$ similarly to Figure 7. Although the sign of the Jacobian in (25) is not obvious in the latter case, we have computed it numerically and confirmed that the Jacobian is strictly positive for the entire solution surface (not shown on figures). Thus, the saddle points of the variational problem (6) are unstable in the time evolution of the mKdV equation (1) according to the instability criterion (25).

3.3. Stability of local minimizers. Local minimizers of the variational problem (6) correspond to the lower solution family on Figure 1. We have checked numerically that the plots of $b = b(c, m)$ versus m for fixed c, $\mathcal{M}(c, m)$ and $\mathcal{F}(c, m)$ versus both c and m are qualitatively

similar to Figures 5, 6, and 7. This is not surprising since the lower and upper solution families are equivalent to each other for $m = 0$.

We have also detected numerically that the Jacobian in the stability criterion (23) remains positive for the entire solution surface. Thus, the local minimizers of the variational problem (6) are stable in the time evolution of the mKdV equation (1) according to the stability criterion (23).

4. Conclusion. The new variational characterization of periodic waves as nondegenerate minimizers of the variational problem (6) has several advantages compared to the previous variational theory, where the energy $E(u)$ is minimized for fixed momentum $F(u)$ and mass $M(u)$. First, the stability criterion is independent of whether the Morse index $n(\mathcal{L})$ is one or two and whether the linear operator $\mathcal{L}$ is degenerate with $z(\mathcal{L}) = 2$. Second, with the exception of the pitchfork bifurcation point $(c, m) = (c_0, 0)$, minimizers of the variational problem (6) are always nondegenerate.

The new variational characterization also has advantages compared to other (partial) characterizations of periodic waves in the mKdV equation such as minimization of energy $E(u)$ for fixed momentum $F(u)$ in [13] or minimization of $B_c(u)$ for fixed L^4 norm in the space of even functions also considered in [18]. The former minimization only allows us to identify a subset of stable periodic waves as it only applies to the periodic waves with $n(\mathcal{L}) = 1$. The latter minimization requires proceeding with an additional Galilean transformation in order to identify the stability criterion for the periodic waves and leads to computational formulas which are not related to the dependence of mass $M(u)$ or momentum $F(u)$ on c.

Although our computations are only based on numerical approximations, the numerical results are rather accurate since we use the exact analytical representations of the periodic wave solutions. We have shown that the periodic waves that correspond to the global and local minimizers of the variational problem (6) are stable in the time evolution of the mKdV equation (1), whereas the periodic waves for the saddle points are unstable.

The main direction to be addressed in further work is to prove analytically that minimizers of the variational problem (6) are nondegenerate in the entire existence interval with the exception of the pitchfork bifurcation point at $(c, m) = (c_0, 0)$. Extensions of these numerical results to the modified Benjamin–Ono equation or the fractional mKdV equation are also of the highest priority. Finally, one can apply the same new variational problem to the generalized fractional KdV equations with powers different from the quadratic and cubic powers considered in [17] and [18], respectively.

REFERENCES

[1] S. Amaral, H. Borluk, G. M. Muslu, F. Natali, and G. Oruc, *On the existence, uniqueness, and stability of periodic waves for the fractional Benjamin-Bona–Mahony equation*, Stud. Appl. Math., 148 (2022), pp. 62–98.

[2] T. P. Andrade and A. Pastor, *Orbital stability of one-parameter periodic traveling waves for dispersive equations and applications*, J. Math. Anal. Appl., 475 (2019), pp. 1242–1275.

[3] J. Angulo, *Non-linear stability of periodic travelling-wave solutions for the Schrödinger and modified Korteweg-de Vries equation*, J. Differential Equations, 235 (2007), pp. 1–30.

[4] J. Angulo and F. Natali, *On the instability of periodic waves for dispersive equations*, Differential Integral Equations, 29 (2016), pp. 837–874.

[5] J. C. Bronski, M. A. Johnson, and T. Kapitula, *An index theorem for the stability of periodic travelling waves of Korteweg-de Vries type*, Proc. Roy. Soc. Edinburgh Sect. A, 141 (2011), pp. 1141–1173.
[6] J. Chen and D. E. Pelinovsky, *Periodic travelling waves of the modified KdV equation and rogue waves on the periodic background*, J. Nonlinear Sci., 29 (2019), pp. 2797–2843.
[7] S. N. Chow and J. A. Sanders, *On the number of critical points of the period*, J. Differential Equations, 64 (1986), pp. 51–66.
[8] B. Deconinck and T. Kapitula, *On the spectral and orbital stability of spatially periodic stationary solutions of generalized Korteweg-de Vries equations*, in Hamiltonian Partial Differential Equations and Applications, Fields Institute Commun. 75, Springer, New York, 2015, pp. 285–322.
[9] B. Deconinck and M. Nivala, *The Stability Analysis of the Periodic Traveling wave Solutions of the mKdV Equation*, Stud. Appl. Math., 126 (2011), pp. 17–48.
[10] L. Gavrilov, *Remark on the number of critical points on the period*, J. Differential Equations, 101 (1993), pp. 58–65.
[11] A. Geyer, R. H. Martins, F. Natali, and D. E. Pelinovsky, *Stability of smooth periodic travelling waves in the Camassa-Holm equation*, Stud. Appl. Math., 148 (2022), pp. 27–61.
[12] R. Grimshaw, *Nonlinear Wave Equations for the Oceanic Internal Solitary Waves*, Stud. Appl. Math., 136 (2016), pp. 214–237.
[13] S. Hakkaev and A. G. Stefanov, *Stability of periodic waves for the fractional KdV and NLS equations*, Proc. Roy. Soc. Edinburgh Sect. A, 151 (2021), pp. 1171–1203.
[14] M. Hărăguş and T. Kapitula, *On the spectra of periodic waves for infinite-dimensional Hamiltonian systems*, Phys. D, 237 (2008), pp. 2649–2671.
[15] V. M. Hur and M. A. Johnson, *Stability of periodic traveling waves for nonlinear dispersive equations*, SIAM J. Math. Anal., 47 (2015), pp. 3528–3554.
[16] M. A. Johnson, *Nonlinear stability of periodic traveling wave solutions of the generalized Korteweg-de Vries equation*, SIAM J. Math. Anal., 41 (2009), pp. 1921–1947.
[17] F. Natali, D. Pelinovsky, and U. Le, *New variational characterization of periodic waves in the fractional Korteweg-de Vries equation*, Nonlinearity, 33 (2020), pp. 1956–1986.
[18] F. Natali, U. Le, and D. E. Pelinovsky, *Periodic waves in the modified fractional Korteweg-de Vries equation*, J. Dynam. Differential Equations, 34 (2022), pp. 1601–1640.
[19] D. E. Pelinovsky, *Localization in Periodic Potentials: From Schrödinger Operators to the Gross-Pitaevskii Equation*, London Math. Soc. Lecture Note Ser. 390, Cambridge University Press, Cambridge, 2011.
[20] D. E. Pelinovsky, *Spectral stability of nonlinear waves in KdV-type evolution equations*, in Nonlinear Physical Systems: Spectral Analysis, Stability, and Bifurcations, O. N. Kirillov and D. E. Pelinovsky, eds., Wiley, London, 2014, pp. 377–400.
[21] E. Pelinovsky, T. Talipova, I. Didenkulova, and E. Didenkulova, *Interfacial long traveling waves in a two-layer fluid with variable depth*, Stud. Appl. Math., 142 (2019), pp. 513–527.
[22] B. R. Sutherland, *Internal Gravity Waves*, Cambridge University Press, Cambridge, 2010.
[23] K. Yagasaki, *Monotonicity of the period function for $u''-u+u^p=0$ with $p\in\mathbb{R}$ and $p>1$*, J. Differential Equations, 255 (2013), pp. 1988–2001.